RSC Advances

PAPER

View Article Online
View Journal | View Issue



Cite this: *RSC Adv.*, 2017, **7**, 47309

# The screening of metal ion inhibitors for glucose oxidase based on the peroxidase-like activity of nano-$Fe_3O_4$

Yao-hui Wu, Lei Chu, Wen Liu, Lun Jiang, Xiao-yong Chen, Yong-hong Wang* and Yun-lin Zhao*

In this study, a colorimetric method is proposed based on the peroxidase-like activity of $Fe_3O_4$ magnetic nanoparticles for screening metal ion inhibitors for glucose oxidase activity. First, the glucose oxidase was typically used as a specific enzyme to catalyze the oxidation of β-D-glucose resulting in the generation of hydrogen peroxide. Next, having an inherent peroxidase-like activity, $Fe_3O_4$ magnetic nanoparticles were adopted as the catalyst. Then, the generated $H_2O_2$ was capable of participating in the oxidation of 3,3′,5,5′-tetramethylbenzidine to yield a blue colored product. Based on the above results, an *in vitro* screen model of metal ion inhibitors of glucose oxidase was thus established. Metal ions including $Ca^{2+}$, $Pb^{2+}$, $Mn^{2+}$, $Ag^{+}$, $Al^{3+}$, $Cu^{2+}$, $Mg^{2+}$ and $Zn^{2+}$ have been tested. Herein, towards the glucose oxidase activity, $Ca^{2+}$, $Pb^{2+}$, $Mg^{2+}$ and $Mn^{2+}$ showed no effect while $Al^{3+}$ and $Zn^{2+}$ displayed a slight activation, while of $Ag^{+}$ and $Cu^{2+}$ expressed a strong inhibition. The further detection of $Ag^{+}$ and $Cu^{2+}$ manifested that their $IC_{50}$ were 0.662 μmol $L^{-1}$ and 12.619 μmol $L^{-1}$, respectively. The entire detection process could be accomplished within 15 min. This assay is economical, time-saving and highly-effective with definitely significant reference for the screening of metal ions as glucose oxidase inhibitors.

Received 26th June 2017
Accepted 13th September 2017

DOI: 10.1039/c7ra07081k

rsc.li/rsc-advances



## 1. Introduction

In terms of environment contamination, metal ions are now ranked one of the most severe contaminants. Among them, lead and mercury[1] are the common heavy metals, which can cause damage to the central nervous system. Lead poisoning can cause a variety of toxic symptoms such as anemia, dizziness, hallucination, headache, insomnia, irritability, weakness of muscles and renal damage. Mercury poisoning causes chest pain, dyspnoea and impairment of pulmonary and kidney function. In addition, the familiar heavy metal ions, cadmium and nickel, are certified as human carcinogens.[2] Cadmium accumulated in the human body can lead to renal dysfunction and in some cases even cause death on high degree of accumulation. High levels of exposure of nickel result in serious lung and kidney problems, such as skin dermatitis, pulmonary fibrosis and gastrointestinal distress. In addition, zinc and copper, which play an important role in the process of growth and development of organisms, bring about serious toxicological problems such as cramps, convulsions and even death on excessive ingestion.[3] The pollution caused by metal ions has been seriously threatening the health of human beings, hence the detection of these metal ions is of increasingly widespread importance.

Many methods have been applied to detect the presence of metal ions, including high performance liquid chromatography (HPLC),[4] thin-layer chromatography (TLC),[5] chemiluminescent immunoassay (CLIA),[6] surface enhanced Raman spectroscopy (SERS),[7] fluorescent spectrometry,[8] electrochemical method[9] and enzyme-inhibition.[10] Among the various methods used for the detection of metal ions thus far, due to its selectivity, the inhibition to enzyme activity offered an appealing choice for the determination of metal ions.[11] Hence, using enzyme-inhibition, the analysis of metal ions attracted a remarkable interest from researchers home and abroad. A variety of enzymes, such as alkaline phosphatase, invertase, catalase, glucose oxidase (GOx) and urease were applied for the detection of metal ions, of which GOx and urease ranked among the most widely reported, showing promise in many cases to be applied for real samples based on the inhibition effect.[12] In particular, initially discovered in *Aspergillus niger* extracts[13] and generally regarded to be one of the most constantly used enzymes in the field of biotechnology, GOx acted as an analytical reagent used for the study of inhibition. Guascito *et al.*[14] used glucose oxidase to successfully develop a screen-printed electrode based amperometric biosensor for the inhibitive detection of heavy metal ions. Rust *et al.*[15] immobilized glucose oxidase on nitrogen-

*Key Laboratory of Forestry Remote Sensing Based Big Data & Ecological Security for Hunan Province, College of Life Science and Technology, Forestry Biotechnology Hunan Key Laboratories, Central South University of Forestry and Technology, 410004, Changsha, China. E-mail: bionano@163.com*

doped carbon nanotubes (N-CNTs) to successfully develop an amperometric glucose biosensor for the determination of silver ions. Ayenimo *et al.*[16] proposed a method describing the detection of $Cu^{2+}$, $Hg^{2+}$, $Cd^{2+}$ and $Pb^{2+}$ through inhibition of the response of an ultrathin polypyrrole–glucose oxidase (PPy–GOx) potentiometric biosensor.

Although the abovementioned biosensor assays used for the inhibitive detection of metal ions were accurate, reproducible and highly specific, it depended on the use of expensive instruments. Compared with biosensor assays, colorimetric assays have attracted considerable interest in metal ions inhibitive detection because of their simplicity, rapid response and cost-effectiveness. GOx could catalyze the oxidation of beta-D-glucose to D-gluconic acid and hydrogen peroxide ($H_2O_2$) with oxygen molecules as electron acceptors.[17] Based on the reaction mechanism of GOx, the glucose–GOx system was usually studied by coupling with a peroxidase-catalyzed color system. Research and development of mimic enzyme have indicated that nanostructured materials as peroxidase mimetics display unparalleled advantages of stability and low-cost compared with natural enzymes,[18] of which magnetic nanoparticles (MNPs) were the most widely studied enzyme mimics. Gao *et al.*[19] have made a surprising discovery that $Fe_3O_4$ MNPs possessed intrinsic peroxidase-like activity. Wang *et al.*,[20] based on the peroxidase-like activity of magnetic mesoporous silica nanoparticles ($Fe_3O_4$@MSN), developed a colorimetric method for the measurement of $H_2O_2$ and glucose.

In this study, we developed a novel model for the screening of metal ion inhibitors of GOx by coupling the glucose–GOx system with the $Fe_3O_4$ MNPs-catalyzed color system. As a mimetic enzyme, it was difficult to deactivate the magnetic nanoparticles, ensuring the stability of the test results. Furthermore, the MNPs could be separated easily by a magnet so that the substances in the solution could be detected conveniently, thus simplifying the operation of the entire detection process. This strategy not only provided a platform for the screening of GOx metal ion inhibitors in a novel, simple and sensitive manner, but also held a huge potential to be utilized in biomolecular diagnosis and studied using other essential enzymes.

# 2. Experimental

## 2.1 Materials

Iron(II) sulfate heptahydrate ($FeSO_4 \cdot 7H_2O$), sodium hydroxide (NaOH), β-D-glucose ($C_6H_{12}O_6 \cdot H_2O$) and potassium hydroxide (KOH) were obtained from Xilong Chemical Reagent Co., Ltd. (Shanghai, China). Hydrogen peroxide ($H_2O_2$, 30%), lead(II) nitrate ($Pb(NO_3)_2$) and silver nitrate ($AgNO_3$) were acquired from Sinopharm Chemical Reagent Co., Ltd. (Shanghai, China). Acetic acid ($CH_3COOH$) and sodium acetate ($CH_3COONa$) were provided by Damao Chemical Reagent Factory (Tianjin, China). Calcium nitrate ($Ca(NO_3)_2 \cdot 4H_2O$), magnesium nitrate ($Mg(NO_3)_2 \cdot 6H_2O$), aluminum nitrate ($Al(NO_3)_2 \cdot 9H_2O$), cupric nitrate ($Cu(NO_3)_2 \cdot 3H_2O$) and zinc nitrate ($Zn(NO_3)_2 \cdot 6H_2O$) were bought from Fengchuan Chemical Reagent Co., Ltd. (Tianjin, China). 3,3′5,5′-Tetramethylbenzidine (TMB) was obtained from Jinsui Biological Technology Co., Ltd. (Shanghai, China). GOx was purchased from Yuanye Biological Technology Co., Ltd. (Shanghai, China). The above regents were analytical or biochemical grade and were used as received. The above solutions were prepared with deionized water. Male healthy urine samples were collected from the volunteers and provided by the Hospital of Central South University of Forestry and Technology. All of the metal ion solutions were diluted with deionized water or male healthy urine.

## 2.2 Instruments

HH-2 digital electric-heated thermostatic water bath (Shanghai, China) was used for controlling the reaction temperature. Pure water preparation system (Qingdao, China) was used to manufacture the deionized water. A JB90-D electric mixer (Shanghai, China) was applied to stir the reaction of synthesizing $Fe_3O_4$ MNPs. A vortex mixer (Labnet International, Inc.) was adopted to mix the reactions. Scanning electron microscope (SEM, Hitachi S-3400N, Japan) was applied to determine the morphology of the MNPs. Magnetic properties of $Fe_3O_4$ MNPs were tested using a vibrating sample magnetometer (VSM, America) and a magnet (NdFeB). The UV-vis absorption and color changes were recorded with a Nanodrop 2000 UV-vis spectrophotometer (Hong Kong, China) and a digital camera, respectively.

## 2.3 Preparation of stock solutions

$FeSO_4 \cdot 7H_2O$ and KOH were dissolved in deionized water with a stock concentration of 0.025 mol $L^{-1}$ and 0.1 mol $L^{-1}$, respectively. The TMB was dissolved in ethanol with a stock concentration of 5 mg $mL^{-1}$. Both $CH_3COOH$ and $CH_3COONa$ were dissolved in deionized water with a stock concentration of 0.2 mol $L^{-1}$ and used with appropriate proportions. The β-D-glucose and all the metal ion salts of crystalline solid were dissolved in deionized water with a stock concentration of 1 mol $L^{-1}$, and used with appropriate dilution. The GOx was dissolved in 0.2 mol $L^{-1}$ acetic acid–sodium acetate buffer solution (pH 4.0) with a stock concentration of 0.25 mg $mL^{-1}$ and placed at 4 °C.

## 2.4 Preparation and characterization of $Fe_3O_4$ MNPs

Mono-dispersed globose $Fe_3O_4$ MNPs were synthesized by a reported sol–gel method.[21] The preparation process consisted of the following steps. First, 200 mL of 0.025 mol $L^{-1}$ $FeSO_4$ solution was added into a beaker. Subsequently, 120 mL of 0.1 mol $L^{-1}$ KOH solution was added. Under the condition that the temperature of the water bath was maintained at 80 °C, 300 μL of 5% $H_2O_2$ solution was rapidly added to the mixture with vigorous stirring for 10 min. The resulting black particles were magnetically separated and repeatedly washed by deionized water and ethanol, in sequence. The $Fe_3O_4$ MNPs were dispersed in 200 mL deionized water, and stored in a narrow-mouth bottle. The morphology and distribution of the product were characterized by a scanning electron microscope (SEM). The magnetic properties of the obtained nanoparticles

 

were verified using a vibrating sample magnetometer (VSM) and a magnet.

### 2.5 Feasibility experiment

A glucose–GOx system was established as a research system. For the glucose–GOx system, 2 mL graduated EP tubes were used as reaction carriers and the reaction volume was defined as 1 mL, including 680 μL of 0.2 mol $L^{-1}$ acetic acid–sodium acetate buffer solution (pH 4.0), 20 μL of 0.25 mg $mL^{-1}$ GOx solution and 300 μL of 0.1 mol $L^{-1}$ glucose solution. Prior to the enzymatic reaction, acetic acid–sodium acetate buffer solution and GOx solution were added into a 2 mL graduated EP tube and preheated for 3 min at a constant temperature of 37 °C in the thermostatic water bath. After the completion of the enzymatic reaction, 500 μL of 1 mol $L^{-1}$ NaOH solution was added into the reaction system for the termination of reaction. The $H_2O_2$ produced in the enzymatic reaction was to be detected.

A color system was established for the detection of the enzymatic reaction produced $H_2O_2$. For the color system, 5 mL graduated EP tubes were used as the reaction carriers and the reaction volume was defined as 3 mL, including 2.1 mL of 0.2 mol $L^{-1}$ acetic acid–sodium acetate buffer solution (pH 3.0), 200 μL $Fe_3O_4$ MNPs dispersion, 100 μL of 5 mg $mL^{-1}$ TMB solution and 600 μL $H_2O_2$ solution from the terminated enzymatic reaction. After reacting for 10 min at room temperature (25 °C), the $Fe_3O_4$ MNPs were magnetically aggregated at the bottom of the EP tube, and thus the supernatant was pipetted for detection. The measurements were conducted with a scan range from 400 nm to 800 nm.

### 2.6 Optimal conditions of enzymatic reaction

In order to understand the relationship between the enzymatic reaction rate and time and obtain the reaction time at which the enzymatic reaction rate was constant, the reactions based on the established glucose–GOx system were carried out from 20 to 300 s and followed the same procedure of detection of $H_2O_2$ based on the established color system. For the glucose–GOx system, the influencing factors involving the concentration of substrate, temperature and pH were optimized. To optimize the substrate concentrations, the series glucose solutions from 0.003 to 0.3 mol $L^{-1}$ were investigated. To optimize the reaction temperature, the reaction solutions incubated in different temperature water baths ranging from 25 to 70 °C were investigated. To optimize the pH of the reaction solution, 0.2 mol $L^{-1}$ acetic acid–sodium acetate buffer solutions with a pH range of 3.0 to 5.0 were investigated. The processes of detection of $H_2O_2$ were similar to that of the feasibility experiment.

### 2.7 Metal ion inhibitors screening

The screening of metal ion inhibitions for GOx was performed based on the optimized enzyme reaction conditions. The effects of different metal ions on the enzymatic activity were investigated. Some ions including $Ca^{2+}$, $Pb^{2+}$, $Mn^{2+}$, $Ag^{+}$, $Al^{3+}$, $Cu^{2+}$, $Mg^{2+}$ and $Zn^{2+}$ were applied in this experiment. The final concentration for each ion was 2 mmol $L^{-1}$. The metal ions that possessed inhibitory effect were screened for further detection. In the screened metal ions detection, five concentration gradients for each ion were prepared through diluting 2 mmol $L^{-1}$ metal ion solution for 10, $10^2$, $10^3$, $10^4$ and $10^5$ times, separately; then the $IC_{50}$ of the metal ion inhibitors were calculated.

### 2.8 Detection of metal ions in urine

The screened metal ions were added to the urine and diluted to the same five concentrations as in the previous experiment. The experimental results were compared with the previous ones.

## 3. Results and discussion

### 3.1 Research strategy

It is generally known that GOx is an ideal enzyme which catalyzes the oxidation of β-D-glucose to D-gluconic and $H_2O_2$ (eqn (1)). Due to its peroxidase-like activity, $Fe_3O_4$ MNPs are able to catalyze the reaction of 3,3′,5,5′-tetramethylbenzidine (TMB) in the presence of $H_2O_2$ to produce a blue color solution (eqn (2)).

$$\text{glucose} + O_2 + H_2O \xrightarrow{\text{GOx}} \text{gluconic acid} + H_2O_2 \quad (1)$$

$$H_2O_2 + \text{TMB} \xrightarrow{Fe_3O_4\ \text{MNPs}} H_2O + \text{oxTMB} \quad (2)$$

We devised a strategy for the screening of GOx metal ion inhibitors based on the above information as shown in Fig. 1. A glucose–GOx system was used as a research system. A color system catalyzed by $Fe_3O_4$ MNPs was established for the detection of $H_2O_2$ produced in GOx-catalyzed reaction. When the color reaction was completed, $Fe_3O_4$ MNPs were magnetically separated using a magnet and the absorbance of the blue product was obtained using a spectrophotometer. The effect of metal ions on GOx activity was investigated based on the change of absorbance before and after GOx was treated with metal ions.

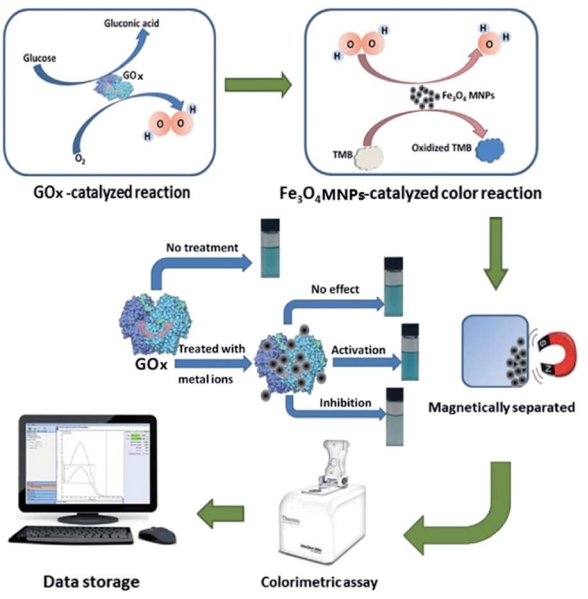


Fig. 1 Schematic illustration of the proposed method for the metal ion inhibitors screening of glucose oxidase.

This was because the activity of GOx was reflected by the absorbance of the blue product. The effect of metal ions on GOx activity was effectively interpreted by the different absorbance of the reaction solutions. Upon treating GOx with metal ions, there could be three possible different results—the ineffective situation, the inhibited situation and the activated situation. We focussed on studying the situation of the inhibitory effect exhibited by the metal ions.

### 3.2 Characterization of $Fe_3O_4$ MNPs and feasibility analysis

To investigate the feasibility of the experiment, we first prepared $Fe_3O_4$ MNPs, and then characterized the morphological structure and magnetic property of the MNPs. The obtained black $Fe_3O_4$ particles were further characterized using scanning electron microscope (SEM) and the recorded image is shown in Fig. 2a. It was observed that the features of the $Fe_3O_4$ particles were homogeneously spherical shaped and the diameter of each particle was about 10 nm. The response of $Fe_3O_4$ particles to the magnetic force was simply tested by a magnet whose results are shown in Fig. 2b. It could be noticed that the originally dispersed black particles rapidly aggregated to the bottom under the action of the magnet. In addition, Fig. 2c displays the magnetization curve for $Fe_3O_4$ MNPs and the values of the saturation magnetization (Ms) and coercive field (Hc) deduced from the measurements are presented in Table 1. It could be easily observed that the magnetization of $Fe_3O_4$ MNPs increased with increasing magnetic field. When the applied magnetic field reached 20 000 kG, the magnetization of the sample saturated and its Ms value obtained was 15.242 emu $g^{-1}$. It was also observed that its Hc was very small, about 5.1474 G, indicating that $Fe_3O_4$ nanoparticles exhibited typical superparamagnetism. Based on the nanometric size and magnetic properties obtained by SEM and VSM, we detected the $H_2O_2$ produced in the GOx-catalyzed reaction using the established $Fe_3O_4$ MNPs-catalyzed color system whose results were shown in Fig. 2c. We found that the $Fe_3O_4$ MNPs catalyzed the reaction of TMB to produce a blue color, with maximum absorbance at 652 nm. This was consistent with the findings of Gao *et al.*[19] This indicated that the prepared $Fe_3O_4$ MNPs indeed exhibited the intrinsic peroxidase-like activity. Hence, the color system catalyzed by $Fe_3O_4$ MNPs was applied for studying the glucose–GOx system. In other words, the feasibility of the experiment was proven.

Table 1 Saturation magnetization and coercive field determined at 300k

| $T$ (K) | Saturation magnetization $M_s$ (emu $g^{-1}$) | Coercive field $H_c$ (G) |
|---|---|---|
| 300 | 15.242 | 5.1474 |

### 3.3 Optimal conditions of enzymatic reaction

In order to ensure that the GOx was the most suitable for playing its catalytic role, we optimized the reaction time, substrate concentration, pH and temperature.

A curve representing the process of GOx-catalyzed reaction was obtained (Fig. 3a) by the reaction from 20 to 300 s. The reaction solutions were measured using a spectrophotometer at 652 nm. From Fig. 3a, it could be observed that the lag phase of the enzymatic reaction process is not clear. This could be caused by the preheating of GOx solution before the reaction. Compared with the lag phase, the linear phase and the nonlinear phase were more evident. From 20 to 60 s, the curve presented a good linear relationship. It was suggested that the

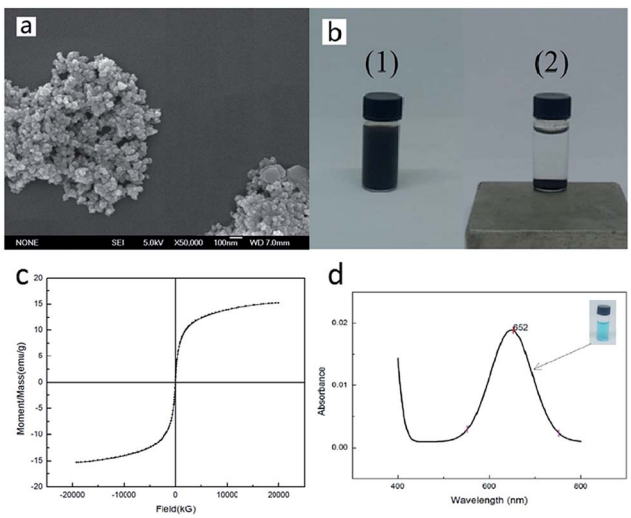


Fig. 2 (a) SEM image of the synthesized $Fe_3O_4$ particles. (b) Response of $Fe_3O_4$ MNPs to a magnet (NdFeB). (1) $Fe_3O_4$ MNPs dispersion liquid. (2) Status that $Fe_3O_4$ MNPs had been gravitated by the magnet. (c) The magnetization curve for $Fe_3O_4$ MNPs. (d) UV-vis absorption spectra (400–800 nm) and the related optical images of the nano-$Fe_3O_4$ catalyzed color reaction.

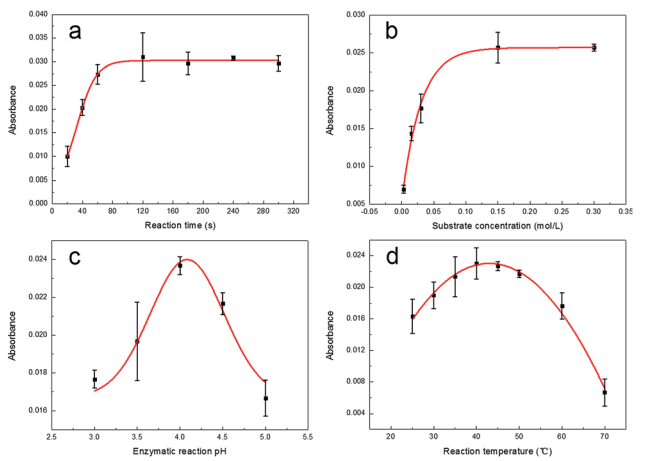


Fig. 3 (a) GOx-catalyzed reaction process curve. The time points are 20, 40, 60, 120, 180, 240 and 300 s. (b) The effect of concentrations of substrate. The concentrations of substrate are 0.003, 0.015, 0.03, 0.15 and 0.3 mol $L^{-1}$. (c) The effect of reaction pH. The pH values are 3.0, 3.5, 4.0, 4.5 and 5.0. (d) The effect of reaction temperatures. The temperatures are 25, 30, 35, 40, 45, 50, 60 and 70 °C.

rate of enzyme reaction was consistent in this period. And with prolonged reaction time, the curve gradually tended to be flat due to several interferences such as inhibitory effect of the product, decrease in the substrate concentration and reduction of the enzyme activity. It could be learned from Fig. 3a that the time for the initial rate of the enzymatic reaction was from 20 to 60 s. In order to set aside enough time for the operation, the reaction time was confirmed as 1 min.

To investigate the effect of substrate concentration on the rate of GOx-catalyzed reaction, we tested through setting up a different substrate concentrations (0.003–0.3 mol $L^{-1}$). From 0.003 to 0.03 mol $L^{-1}$, the relationship between the reaction rate and the substrate concentration was proportional (Fig. 3b). This indicated that the enzymatic reaction was manifested as a first-order reaction. From 0.03 to 0.15 mol $L^{-1}$, the increase in enzyme reaction rate was not proportional to the concentration (Fig. 3b). This showed that the enzymatic reaction was manifested as a mixed-order reaction. When the substrate concentration exceeded 0.15 mol $L^{-1}$, the rate of enzymatic reaction was independent of the substrate concentration (Fig. 3b). This suggested that the enzymatic reaction was manifested as a zero-order reaction. This occurred because the GOx in the solution were completely saturated with the substrate so that there was no excess enzyme in the solution. Although the substrate concentration was increased, no more intermediates were produced. It was clear that the enzymatic reaction reached its maximum reaction rate ($V_{max}$) at a substrate concentration of 0.15 mol $L^{-1}$. Therefore, the optimum substrate concentration was determined to be 0.15 mol $L^{-1}$.

To investigate the effect of pH on the rate of GOx-catalyzed reaction, we tested through setting up different pH ranging from 3 to 5. The resultant curve obtained is shown in Fig. 3c, which is a bell-shaped curve and revealed that GOx exhibited the highest catalytic activity at pH 4.0. This was because the dissociation state of GOx at pH 4.0 was most favorable for the combination with the substrate, while other pH affected the conformation of the enzyme active site that affected the binding to the substrate. Thus, pH 4.0 was fixed as the optimum pH.

To investigate the effect of temperature on the rate of GOx-catalyzed reaction, we tested through setting up different temperatures ranging from 25 to 70 °C. As shown in Fig. 3d, from 25 to 40 °C, the rate of enzymatic reaction accelerated with the increase in temperature. The reason was that the denaturation of GOx had not yet been observed at the range below its optimum temperature. However, from 40 to 70 °C, the rate of enzymatic reaction reduced with the increase in temperature. This was because GOx started to denaturate when the temperature was higher than its optimum temperature. The effect that the enzymatic reaction rate accelerated with increase in temperature was counteracted by the influence of GOx denaturation. Thus, the rate of enzymatic reaction rapidly decreased. According to the above analysis, the optimum temperature was 40 °C. The optimum conditions for the GOx-catalyzed enzymatic reaction are listed in Table 2.

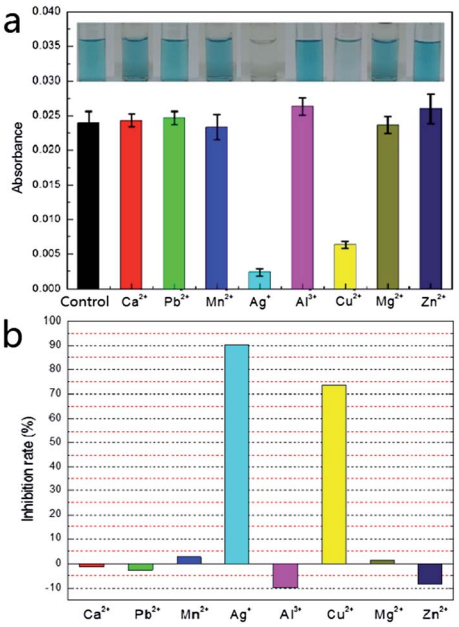


Fig. 4 The screening of GOx metal ion inhibitors. (a) UV-vis absorption spectra (652 nm) and the related optical images of control group (GOx untreated by metal ions) and experimental groups (GOx treated by metal ions). (b) Effects of metal ions (2 mM) on GOx activity. The metal ions are $Ca^{2+}$, $Pb^{2+}$, $Mn^{2+}$, $Ag^{+}$, $Al^{3+}$, $Cu^{2+}$, $Mg^{2+}$ and $Zn^{2+}$.

### 3.4 Metal ion inhibitors screening

In order to examine the possibility of screening for GOx metal ion inhibitors, we analyzed the effects of several metal ions on the enzyme. The screening in the presence of metal ion inhibitors was investigated using the optimal enzymatic reaction conditions obtained above. As shown in Fig. 4a, the measured absorbance was significantly lower than the control (GOx untreated by metal ions) when GOx was treated by $Ag^{+}$ and $Cu^{2+}$; when GOx was treated by $Ca^{2+}$, $Pb^{2+}$, $Mn^{2+}$, $Al^{3+}$, $Mg^{2+}$ and $Zn^{2+}$, the measured absorbance was similar to that of the control. The influencing degree of metal ions on GOx could be calculated from Fig. 4a and the results are displayed in Fig. 4b. It is clear that except $Ag^{+}$ and $Cu^{2+}$, other metal ions had no significant inhibitory effect on GOx activity. This was consistent with the previous reports.[22,23] Besides, the metal ions except $Ag^{+}$ and $Cu^{2+}$, $Ca^{2+}$, $Pb^{2+}$, $Mg^{2+}$ and $Mn^{2+}$ showed no effect on GOx activity, while $Al^{3+}$ and $Zn^{2+}$ expressed a slight activation. $Ag^{+}$ and $Cu^{2+}$ could prevent the reduced form of the flavin cofactor

Table 2 Optimal conditions of the GOx-catalyzed reaction

| | Reaction time (min) | Substrate concentration (mol $L^{-1}$) | pH | Temperature (°C) |
|---|---|---|---|---|
| Optimum conditions | 1 | 0.15 | 4.0 | 40 |

($FADH_2$) from reducing the electron acceptor so that the GOx activity was inhibited. This explanation is based on the study reported by Wang *et al.*,[22] showing that GOx inhibition by metal ions was closely linked with the coordination of the reduced form of the flavin cofactor ($FADH_2$) in the active site of GOx with the metal ion.

### 3.5 The detection of metal ions

In order to further confirm our results, we used $Ag^+$ and $Cu^{2+}$ to study their inhibitory effect. In the test, both $Ag^+$ and $Cu^{2+}$ were diluted 10 times, $10^2$ times, $10^3$ times, $10^4$ times and $10^5$ times on the basis of 2 mmol $L^{-1}$. Then the inhibition efficiency curves for $Ag^+$ (Fig. 5a) and $Cu^{2+}$ (Fig. 5b) were obtained and their $IC_{50}$ were respectively measured as 0.662 μmol $L^{-1}$ and 12.619 μmol $L^{-1}$. The $IC_{50}$ value for $Ag^+$ was significantly smaller than that for $Cu^{2+}$, indicating that $Ag^+$ displayed a stronger inhibitive effect compared with $Cu^{2+}$. This is in agreement with the literature results.[22,23] The only difference was that the $IC_{50}$ value for $Ag^+$ and $Cu^{2+}$ measured in our study were about 100 times lower than those obtained by Wang *et al.*[22]

In order to verify whether our detection method could be applied to a certain live sample, the standard addition method was used to add the metal ion inhibitors to the urine and the urine samples were measured by the same method as discussed in an earlier section (2.7 Metal ion inhibitors screening). The measured results were compared with the previous data (as shown in Fig. 6). From Fig. 6, it could be seen that for the absorbance, the measured value of the standard sample and the urine sample were not much different, indicating that the system established in our study could be applied to actual samples.

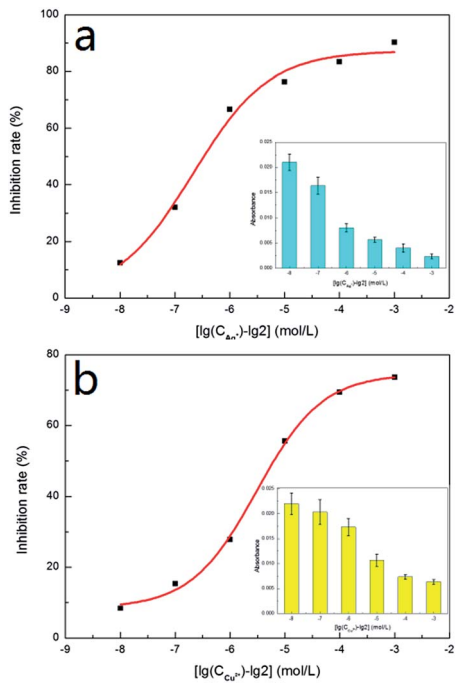


Fig. 5 The detection of screened out metal ions. (a) The effect of different concentrations of $Ag^+$ on GOx activity, a series of concentrations of $Ag^+$ ranging from $2 \times 10^{-8}$ to $2 \times 10^{-3}$ mol $L^{-1}$. (b) The effect of different concentrations of $Cu^{2+}$ on GOx activity, a series of concentrations of $Cu^{2+}$ ranging from $2 \times 10^{-8}$ to $2 \times 10^{-3}$ mol $L^{-1}$.

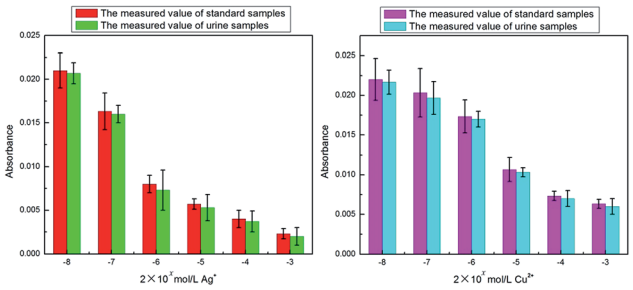


Fig. 6 The comparison of absorbance measured by standard samples and urine samples.

## 4. Conclusions

A new type of *in vitro* screening pattern had been developed, based on the peroxidase-like activity of nano-$Fe_3O_4$. Using the established screening pattern, the metal ion inhibitors of GOx were successfully screened and detected. Our detection method used TMB as the color reagent and $Fe_3O_4$ MNPs which were not easily deactivated compared to the natural peroxidase, hence it had a good visual effect and stability in the test results. Furthermore, the proposed assay whose entire detection process was completed within 15 min is rapid and the detection limit measured could reach the levels of $10^{-2}$ micromoles per liter. However, although our system could recognize and determine a variety of different single metal ion inhibitors, it could determine mixed metal ion inhibitors. Even so, the new *in vitro* screening model established in our study is efficient, accurate and repeatable. Referring to this approach, a framework could be provided for the development of many different screening patterns of enzyme inhibitors.

## Ethical statement

Male healthy urine samples were provided by the Hospital of Central South University of Forestry and Technology. The collected urine samples were not allowed to be used for purposes other than those used in our project. Under this condition, the Hospital agreed that the collected urine samples could be used in our project. The content and process of the study followed the international and national promulgated ethical requirements for biomedical research. All study participants provided informed consent.

## Conflicts of interest

There are no conflicts to declare.

## Acknowledgements

This study is supported in part by the Research Foundation of Education Bureau of Hunan Province, China (Grant No. 16A227) Key Technology R&D Program of Hunan Province (2016TP1014, 2016TP2007).

## Notes and references

1 (*a*) F. Fu and Q. Wang, *J. Environ. Manage.*, 2011, **92**, 407; (*b*) R. Naseem and S. S. Tahir, *Water Res.*, 2001, **35**, 3982; (*c*) C. Namasivayam and K. Kadirvelu, *Carbon*, 1999, **37**, 79.

2 C. E. Borba, R. Guirardello, E. A. Silva, M. T. Veit and C. R. G. Tavares, *Biochem. Eng. J.*, 2006, **30**, 184.

3 (*a*) N. Oyaro, O. Juddy, E. N. M. Murago and E. Gitonga, *J. Food, Agric. Environ.*, 2007, **5**, 119; (*b*) A. T. Paulino, F. A. S. Minasse, M. R. Guilherme, A. V. Reis, E. C. Muniz and J. Nozaki, *J. Colloid Interface Sci.*, 2006, **301**, 479.

4 G. Yang, Z. Li, H. Shi and J. Wang, *J. Anal. Chem.*, 2005, **60**, 480.

5 K. T. D. Bleyker and T. R. Sweet, *Chromatographia*, 1980, **13**, 114.

6 (*a*) E. P. Borges, A. F. Lavorante and B. F. D. Reis, *Anal. Chim. Acta*, 2005, **528**, 115; (*b*) H. Z. He, K. H. Leung, H. Yang, S. H. Chan, C. H. Leung and J. Zhou, *Biosens. Bioelectron.*, 2013, **41**, 871.

7 K. Carron, K. Mullen, M. Lanouette and H. Angersbach, *Appl. Spectrosc.*, 1991, **45**, 420.

8 (*a*) S. Sahana and P. K. Bharadwaj, *Inorg. Chim. Acta*, 2014, **417**, 109; (*b*) K. Varazo, C. L. Droumaguet, K. Fullard and Q. Wang, *Tetrahedron Lett.*, 2009, **50**, 7032.

9 (*a*) S. Williams, A. Zhou, H. Zhang and W. Zhang, *J. Electrochem. Soc.*, 2015, **148**, C709; (*b*) C. Yamamoto, H. Seto, K. Ohto, H. Kawakita and H. Harada, *Anal. Sci.*, 2011, **27**, 389; (*c*) M. Li, D. W. Li, Y. T. Li, D. K. Xu and Y. T. Long, *Anal. Chim. Acta*, 2011, **701**, 157.

10 (*a*) L. Campanella, G. Favero, M. Tomassetti and A. Torresi, *Curr. Top. Anal. Chem.*, 2005, 1; (*b*) Y. Hua, *Shanghai Environ. Sci.*, 2003, **22**, 939–942.

11 B. K. Bansod, T. Kumar, R. Thakur, S. Rana and I. Singh, *Biosens. Bioelectron.*, 2017, **94**, 443.

12 (*a*) L. K. Shyuan, L. Y. Heng, M. Ahmad, S. A. Aziz and Z. Ishak, *Asian J. Biochem.*, 2008, **3**, 359; (*b*) H. Mohammadi, A. Amine, S. Cosnier and C. Mousty, *Anal. Chim. Acta*, 2005, **543**, 143; (*c*) E. Akyilmaz and O. Kozgus, *Food Chem.*, 2009, **115**, 347; (*d*) M. E. Ghica and C. M. A. Brett, *Mikrochim. Acta*, 2008, **163**, 185; (*e*) B. Kuswandi, *Anal. Bioanal. Chem.*, 2003, **376**, 1104; (*f*) P. Pal, D. Bhattacharyay, A. Mukhopadhyay and P. Sarkar, *Environ. Eng. Sci.*, 2009, **26**, 25; (*g*) Z. Wen, S. Ci and J. Li, *J. Phys. Chem. C*, 2009, **113**, 13482; (*h*) T. K. V. Krawczyk, M. Moszczyńska and M. Trojanowicz, *Biosens. Bioelectron.*, 2000, **15**, 681.

13 C. M. Wong, K. H. Wong and X. D. Chen, *Appl. Microbiol. Biotechnol.*, 2008, **78**, 927.

14 M. R. Guascito, C. Malitesta, E. Mazzotta and A. Turco, *Sens. Lett.*, 2009, **7**, 153.

15 I. M. Rust, J. M. Goran and K. J. Stevenson, *Anal. Chem.*, 2015, **87**, 7250.

16 J. G. Ayenimo and S. B. Adeloju, *Talanta*, 2015, **137**, 62.

17 D. G. Hatzinikolaou and B. J. Macris, *Enzyme Microb. Technol.*, 1995, **17**, 530.

18 Y. Guo, L. Deng, J. Li, S. Guo, E. Wang and S. Dong, *ACS Nano*, 2015, **5**, 1282.

19 L. Gao, J. Zhuang, L. Nie, J. Zhang, Y. Zhang and N. Gu, *Nat. Nanotechnol.*, 2007, **2**, 577.

20 Y. Wang, B. Zhou, S. Wu, K. Wang and X. He, *Talanta*, 2015, **134**, 712.

21 O. M. Lemine, K. Omri, B. Zhang, L. E. Mir, M. Sajieddine and A. Alyamani, *Superlattices Microstruct.*, 2012, **52**, 793.

22 S. Wang, P. Su and Y. Yang, *Anal. Biochem.*, 2012, **427**, 139.

23 (*a*) M. T. Meredith and S. D. Minteer, *Anal. Chem.*, 2011, **83**, 5436; (*b*) C. Chen, Q. Xie, L. Wang, C. Qin, F. Xie and S. Yao, *Anal. Chem.*, 2011, **83**, 2660.